International Journal of Mechanical and Materials Engineering (IJMME), Vol. 5 (2010), No.2, 260-267

CRUSH SIMULATION OF WOVEN C-GLASS/EPOXY UNMANNED ARIEL VEHICLE FUSELAGE SECTION

N. Yidris, R. Zahari, D.L. Majid, F. Mustapha, M.T.H. Sultan and A.S.M. Rafie
Department of Aerospace Engineering, Faculty of Engineering, University Putra Malaysia
43400 UPM, Serdang Selangor, Malaysia
E-mail: rizal@eng.upm.edu.my/rizal666@yahoo.com

Received 22 September 2009, Accepted 12 August 2010

ABSTRACT

A quasi-static crush analysis of an unmanned aerial vehicle (UAV) fuselage section made of woven c-glass/epoxy has been conducted using the finite element simulation via ABAQUS. The main material and strength properties of the c-glass/epoxy (200 g/m^2) which were needed in the ABAQUS analyses were obtained from standard material characterization tests. A progressive damage methodology using ABAQUS has been employed in order to simulate the non-linear material behaviour of the composite fuselage section. Two stress based failure theories were programmed in the user subroutine code (USDFLD) and linked with ABAQUS in order to predict the damage of the composite materials. Satisfactory level of agreement between simulation and test results were obtained regarding the main crushing characteristics of the tested woven c-glass/epoxy fuselage sections such as peak compressive load, crush energy absorption and the overall crushing response. It has been observed that the predicted peak load are found to agree with the experimentally recorded peak load within an accuracy of 3.44% and 4.09% for Tsai-Hill and Tsai-Wu Failure criterion, respectively. In addition, the simulated crushing energy absorption results show reasonable accuracy with the experimental values. This confirms the accuracy of the progressive damage methodology implemented in FE analysis for the woven glass/epoxy fuselage sections.

***Keywords*:** Crush analysis; Woven Glass/epoxy; Progressive damage analysis; Stresses based failure theory; UAV fuselage section

1. INTRODUCTION

Over the past decade, UAVs have been in operation around the world. Many countries are working to increase the capabilities of existing unmanned systems and to develop new systems with improved capabilities. In general the purpose of an unmanned aerial vehicle is to carry out various operations for which the UAV is designed to accomplish such as scientific reconnaissance role, mapping, military survey, carrying weapons and lunching weapons, surveillance of borders and coasts, fire detection, search and rescue, etc. UAVs can generally be categorized as tactical, endurance, vertical takeoff and landing (VTOL), man portable, or hand-launched, optionally piloted vehicles (OPVs), micro air vehicles (MAVs), and research (the UAV equivalent of X-planes). In general, UAV structures have the same function as aircraft structures that are to transmit and resist the applied loads with zero or allowable deflection. During flight the structures must maintain the design aerodynamic shape and must safely protect the payload, instrument, systems from environmental conditions and acceptable crash conditions.

The use of composite materials in UAV structural design is nowadays extremely attractive due to their considerable strength-to-weight ratio. The monocoque structure type is chosen for the UAV fuselage because of mostly the ease of fabrication using composite and the gain in useful area in the fuselage. The capacity and behavior of composite shells to withstand loads is of fundamental interest as thin-walled shells have constituted primary structural parts of aircraft construction for many years. Nowadays, UAV carries not only flying equipment such as servo motors but also expensive instruments which could cost millions such as state-of-the-art cameras. These instruments help UAV carry out various operations for which the UAV is designed for. Therefore, it is believed that energy absorption and crashworthiness applies not only to manned aircraft but also unmanned aircraft and it will become a significant consideration in UAV design in the near future. A series of laboratory investigations and simulations were carried out at NASA Langley Research Center to develop a new fuselage concept (Jackson, 1996, 1997). The development of an innovative composite fuselage concept for light aircraft and rotorcraft was carried out by Jackson and Fasanella (1998). The fuselage concept was designed and evaluated during the first two years of the research program. In the third year of the research program, a full-scale prototype was fabricated, tested and compared with the behavior of the 1/5-scale model fuselage. The advantages of the new fuselage concept and tests conducted to verify compliance with structural and flight load requirements (Jackson and Fasanella, 1998a, b, c, 1999).

In the three year research program, Jackson (1997) only did two tests on the upper part of the fuselage. The tests were structural stiffness test and internal pressure test. In the structural stiffness test, the structural stiffness data

provided valuable insight concerning the effective modulus of the composite material used to construct the section. In the internal pressure test, the fuselage section was pressurized with water. The goal was to satisfy or exceed a 10 psi internal pressure, while maintaining floor rigidity (mid-point floor displacement equal to or less than 0.1 inch).

Vertical drop tests of a composite fuselage concept were also conducted at both 0^o –roll and 15^o –roll impact attitudes to evaluate the crashworthy features of the fuselage design (Jackson and Fasanella, 2000). During the 15^o –roll vertical drop test, no observable rebound of the fuselage occurred but damage to the fuselage occurred in the transition region between the curved upper section and the floor on both sides. The damage on the right side, however, was much more severe. The upper section was designed to be relatively rigid and the research did not consider the upper side crash condition.

To date, no work was reported which study the effect of transverse load applied onto the fuselage upper section numerically. It is therefore important to carry out the study of the capability of the upper section part in absorbing crash load which is the main objective of this work. In this present research work the fuselage section shape adopted is based on the works carried out by Jackson and Fasanella (1998) research only that it is applied to a typical unmanned aerial vehicle (UAV).

2. QUASI STATIC CRUSHING TEST

The fuselage specimens were fabricated using a piece of custom-built mandrel, or mold, which is shown in Figure 1. The cross section and the dimension of the mandrel are shown in Figure 2. To demonstrate the low-cost fabrication process used in this study the fuselage sections have been constructed using woven c-glass/epoxy in normal room condition and without the use of special and costly equipment such as the autoclave. A woven C-glass/epoxy composite material was chosen because of its low cost and commercially available. The fuselage section was oriented at 45/-45/90/0 with respect to the cylinder axis as shown in Figure 3. The quasi-isotropic laminate stacking sequence was selected as it has the orientation in major direction.
C-glass fabric, type $200g/m^2$, was used as the reinforcing media. The first stage in the fabrication process was to prepare the c-glass fabric with the entire orientation angle. The process began with laying the c-glass woven fabric on a table which then was marked using the marker pen and the protector. The protector was used to mark the orientation angle. After all the marking were set the cloth was cut using a tailor scissor as shown in Figure 4. The second stage was preparing the surface of the mandrel. The mandrel was placed on the holding jig and polished with the mold release wax in several coatings. The mold release wax functioned as a release agent and the coating layers separated the cured composite with the mandrel.

Figure 1: The mandrel and the aluminum outer cover

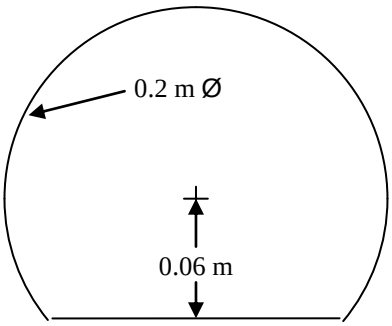

Figure 2: Dimension of the fuselage section

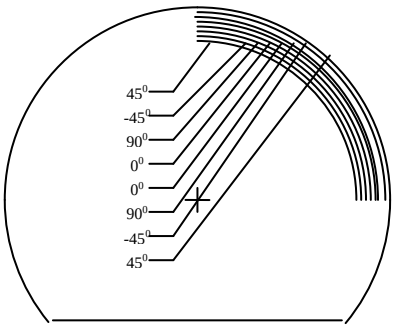

Figure 3: Schematic drawing of the fuselage construction process

Figure 4: C-glass woven fabric cloth

All of the previous procedure must have been ready before the third stage began which was epoxy resin preparation. EP 215A with curing agent EP 215 B (weight ratio of resin/curing agent = 4:1), a room temperature curing epoxy resin, was used as the matrix material. The mixed epoxy solution was stirred using electric stirrer in order to get good mixture.

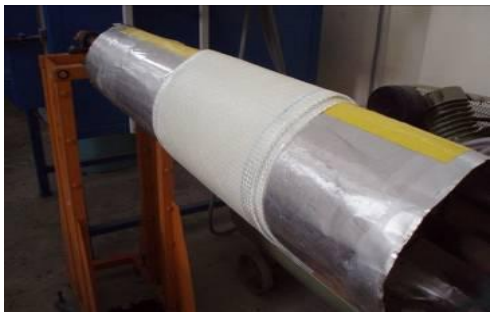

Figure 5: C-glass/epoxy cloth wrapped around the mandrel

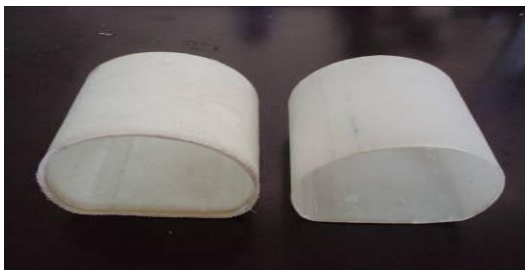

Figure 6: The cured composite fuselage section of type 200g/m^2

Figure 7: Quasi-static testing using MTS machine

The fourth stage was fabricating the fuselage specimen which consisted of eight layers orientated at different angles. Each layer of c-glass fabric skin and epoxy resin was sequentially wrapped and poured around the mandrel as shown in Figure 5. All curing was performed under ambient pressure at room temperature. The final stage was to separate the finished part from the mandrel. The finished fuselage specimen is shown in Figure 6. The quasi-static crushing test was performed by the Universal Testing Machine (UTM). The testing machine heads comprised of a stationary head and a moveable head. The drive mechanism was capable of imparting to the moveable head a controlled velocity 10 mm/min with respect to the stationary head. The load-sensing device was capable of indicating the total load being carried by the test specimen. The grip of each head held the anvil so that the direction of the load applied to the specimen was coincident with the transverse axis of the specimen. Figure 7 shows the arrangement of the fuselage section on the testing area.

3. MATERIAL CHARACTERIZATION PROCEDURE

The material characterization procedure determines the in-plane tensile modulus of elasticity (E_{11} & E_{22}), in-plane shear modulus (G_{12}), Poisson's ratio (ν), ultimate tensile strength, ultimate tensile strain, and ultimate shear strength of polymer matrix composite materials reinforced by high-modulus fibers. Most testing methods used. The laminate of the tested specimens was a balanced type and symmetric with respect to the test direction which conformed to the ASTM (ASTM D 3039, ASTM E 111, ASTM E 1237 and ASTM E132).

The apparatus needed in preparing the thin flat strip of composite material are voltmeter, emery clothes, super glue, vernier caliper, micrometer, strain gages and strain gage cement. The voltmeter was used to test that the wires used for strain gages were in good condition. Emery cloths of sizes 46 for tabbing and 1000 for surface preparation were used on the specimen. Super glue was used as an adhesive for the emery cloth. The vernier caliper and micrometer were used to measure the width and the thickness of the specimen respectively. Strain gages of type KFRP which is suitable for composite materials and strain gage cement of type CC-33A were the sensors to measure the strain.

In general two flat plates of c-glass/epoxy of type 200g/m^2 was cut into coupon specimens 250 mm long and 25 mm wide, with the fabric warp direction parallel to the sample longitudinal direction. The entire specimens were instrumented with strain gages and tested in tensile to provide stress-strain response as shown in Figure 8.

Figure 8: Coupon specimens for tensile testing

The general test method recommended for tensile strength is ASTM D3039 Test Method for Tensile Properties of Fiber-Resin Composites (ASTM D3039). UTM machine was used to conduct the test for c-glass/epoxy 200g/m^2 type specimens as shown in Figure 9. Tensile test specimen for finding the longitudinal

tensile strength consisted of eight plies of 0^0 directions. The specimen was instrumented with strain gages in the longitudinal and transverse direction, which is shown in Figure 10.

Figure 9: UTM machine for tensile testing

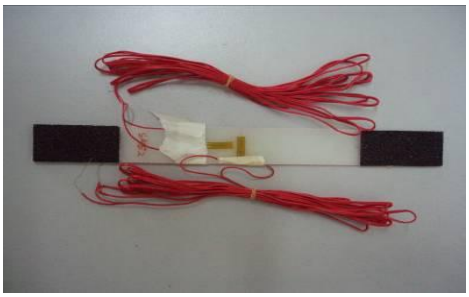

Figure 10: Specimen with the mounted longitudinal and transverse strain gages

The coupon specimen was then mounted in the grips of the UTM machine and monotonically loaded in tension while recorded load as shown in Figure 11. Tensile stresses were applied on the specimen at a rate of 1 mm/min. The ultimate strength of the material was determined from the maximum load carried prior to failure. Load-displacement response of the material was monitored and recorded, from which the ultimate tensile stress, ultimate tensile strain, tensile modulus of elasticity, and Poisson's ratio were derived.

Figure 11: Specimen in the grip of UTM machine

A total of 230 to 260 data points for load and displacement were taken until the specimen failed. Equipment used for recording the data was the Wheatstone bridge box, strain amplifier equipment and data acquisition card. The stress in the longitudinal direction was plotted as a function of longitudinal strain.

The procedure for finding the transverse tensile strength was the same as for finding the longitudinal tensile strength only that a single strain gage was used. Figure 12 shows the coupon specimen for transverse tensile testing.

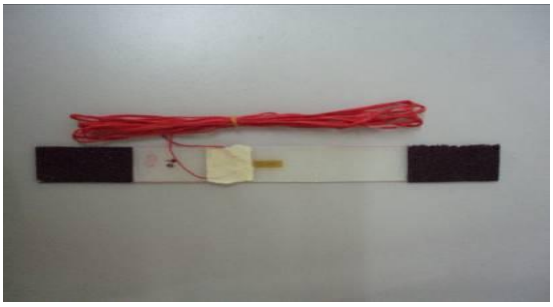

Figure 12: Coupon specimen for determining the transverse tensile property

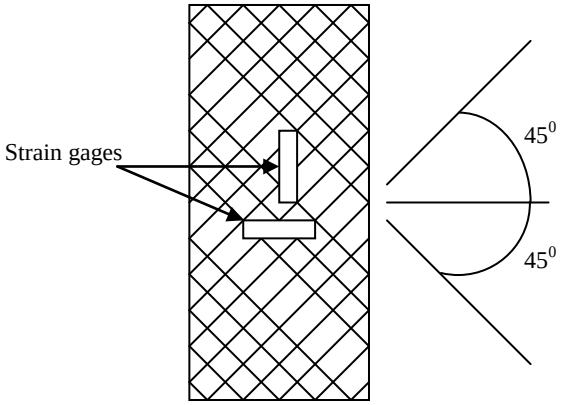

Figure 13: Schematic of a $[45/-45]_{2s}$ laminate shear test

Method for obtaining the in-plane shear strength is the $[+/-45]_{2s}$ laminated tensile coupon loaded in tension (Figure 13). A $[+/-45]_{2s}$ laminate is an 8-ply laminate with [+45/-45/+45/-45/-45/+45/-45/+45] distribution of plies on top of each other. An axial stress is applied to the 8-ply laminate and the axial and transverse strains, respectively, were measured. From the mechanical characterization tests, the summary of the obtained properties for type the woven C-glass/epoxy 200g/m^2 is as Table 1.

Table 1: Summary of mechanical properties for C-glass/epoxy 200g/m^2

Properties	**C-glass/Epoxy 200g/m^2**
E_{11}	12.246 GPa
E_{22}	11.339 GPa
v_{12}	0.158
G_{12}	2.340 GPa
$(\sigma_1^T)_{ult}$	181.552 MPa
$(\varepsilon_1^T)_{ult}$	0.023293 mm/mm
$(\sigma_2^T)_{ult}$	172.462 MPa
$(\varepsilon_2^T)_{ult}$	0.023089 mm/mm
$(\sigma_{12})_{ult}$	39.626 MPa

4. FAILURE THEORIES FOR COMPOSITES

The strength of a laminate is related to the strength of its individual lamina. Various failure theories for composite structures have been developed for predicting when a failure has occurred. These theories are needed in order to compare the state of stress in an element to the failure criterion. In this paper, two failure theories namely, Tsai-Hill failure theory (Tsai and Wu, 1971, 1948) failure theory are employed in the material degradation model. The compressive strength parameters of the c-glass/epoxy composite have never been published elsewhere and are unknown at this time. Consequently, the assumption that $(\sigma^C{}_1)_{ult}$ equals $(\sigma^T{}_1)_{ult}$ and $(\sigma^C{}_2)_{ult}$ equals $(\sigma^T{}_2)_{ult}$ has been made.

$$\left[\frac{\sigma_1}{\left|\sigma_1^T\right|_{ult}}\right]^2 - \left[\frac{\sigma_1\sigma_2}{\left|\sigma_1^T\right|^2_{ult}}\right] + \left[\frac{\sigma_2}{\left|\sigma_2^T\right|_{ult}}\right]^2 + \left[\frac{\tau_{12}}{\left|\tau_{12}\right|_{ult}}\right]^2 < 1 \quad (1)$$

As the compression strength is assumed to be equivalent to tensile strength the Tai-Wu theory can be expressed as follows.

In Tsai-Hill failure theory, failure occurs when the distortion energy of an element is greater than the failure distortion energy of the material. The theory states that if equation (1) is violated failure has occurred in the element.

$$\left[\frac{\sigma_1^2}{\left|\sigma_1^T\right|^2_{ult}}\right] + \left[\frac{\sigma_2^2}{\left|\sigma_2^T\right|^2_{ult}}\right] + \left[\frac{\tau_{12}^2}{\left|\tau_{12}\right|^2_{ult}}\right] - \left[\sigma_1\sigma_2\sqrt{\frac{1}{\left|\sigma_1^T\right|^2_{ult}\left|\sigma_2^T\right|^2_{ult}}}\right] < 1 \quad (2)$$

5. PROGRESSINVE FAILURE METHODOLOGY

In order to simulate non-linear material bahaviour in composite structures a progressive damage methodology has been implemented in the finite element analysis of the fuselage structures. Each of the failure theory algorithms was coded in the ABAQUS/Standard user subroutine USDFLD (ABAQUS, 2003) which was linked with the nonlinear analysis. The elastic material properties were made to depend on the field variables which themselves can be a function of any Gauss point quantity such as stress, strain, etc.. In this material degradation model, all of the elastic materials properties are reduce to zero once the failure criteria are met. The progressive damage flowchart is shown in figure 14. Plane stresses from the previous increment are called into the subroutine at the start of the current increment and used to evaluate any of the failure criteria stated in Eqs (1) and (2). Once the failure criteria are met, the field variables are updated and used to reduce the material properties to zero of their original value according to the scheme shown in table 2.

The redefinition of field variables is local to the current increment so any history dependence must be introduced with user-defined state-variables that can also be updated in USDFLD. History dependence is very crucial for progressive damage modelling because once failure is detected at a gauss point, it must remain in that condition and must not 'heal' after the stresses are re-distributed.

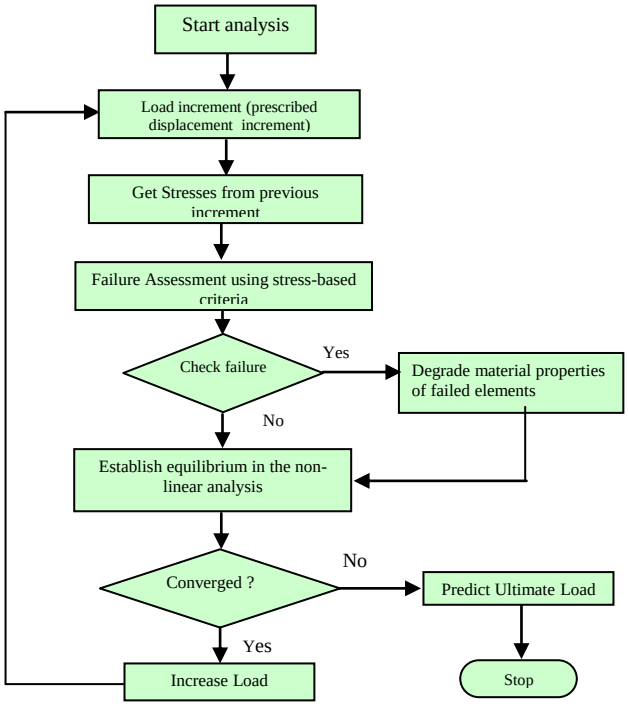

Figure 14 Progressive damage algorithm

Table 2 Dependence of the elastic material properties on the field variables

Material state	Elastic Mechanical Properties				Field Variables
No failure detected	E11	E22	V12	G12	0
Failure at material (Gauss) point	0	0	0	0	1

6. FINITE ELEMENT MODEL DEVELOPMENT

The simulation of the crushing behavior of a fuselage section uses contact modeling techniques and user subroutine code for obtaining a successful contact analysis and damage analysis in ABAQUS/Standard. The problem consists of a shell of deformable material, called the fuselage section, and the tools which are the moveable anvil and the stationery anvil that are in contact with the top and bottom of the fuselage section respectively. The tools are modeled as rigid surfaces

because they are much stiffer than the fuselage section. Figure 15 shows the schematics of the arrangement of the components.

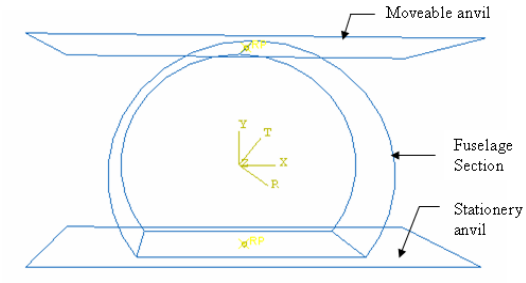

Figure 15: Schematic drawing of the fuselage and boundary conditions

The deformable structure is made of eight-layered composite shell that is simply supported at the bottom surface. The movable anvil modeled as rigid plate will crush the fuselage laterally from the top surface of the fuselage section. The layers are oriented at $[45/-45/90/0]_s$ with respect to the longitudinal axis. Figure 16 shows the ABAQUS finite element model of the UAV fuselage section. The model consists of 2612 nodes and 2523 S4R (4-noded shell element with reduced integration) shell elements. The material properties entered into ABAQUS/Standard code were determined from experimental data of the previous material characterization tests.

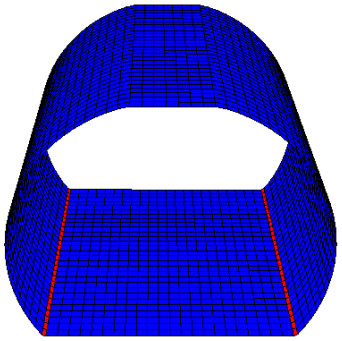

Figure 16 Mesh of the deformable fuselage section

6.1 Mesh Convergence study

A mesh convergence study was conducted to ensure that the results obtained from ABAQUS simulation are reliable and accurate. Coarse meshes usually yield inaccurate results. As the mesh density increases the numerical solution will tend toward converged values. Nine different mesh densities were used and the influence of the mesh density on two particular results is compared in Table 3. The convergence of the results is plotted in Figure 17 and Figure 18. The coarse mesh predicts inaccurate results but as the meshes are refined all predict similar results. All the results are normalized with respect to the values predicted by the coarse mesh. From the study, 2523 S4R shell elements have been chosen as the number of elements needed to produce reliable results throughout the analysis.

Table 3: Results of mesh convergence study

No. of element	Tsai-Hill		Tsai-Wu	
	Peak load, N	Energy absorbed, J	Peak load, N	Energy absorbed, J
533	1366	78.36	1366	78.36
616	1683	85.43	1683	85.97
720	1856	98.07	1856	98.33
1008	1818	95.36	1848	96.72
1121	1800	93.68	1814	93.95
1240	1380	78.98	1388	72.83
1496	1598	86.57	1612	83.67
1925	1591	88.22	1603	88.35
2523	1593	88.11	1603	86.35

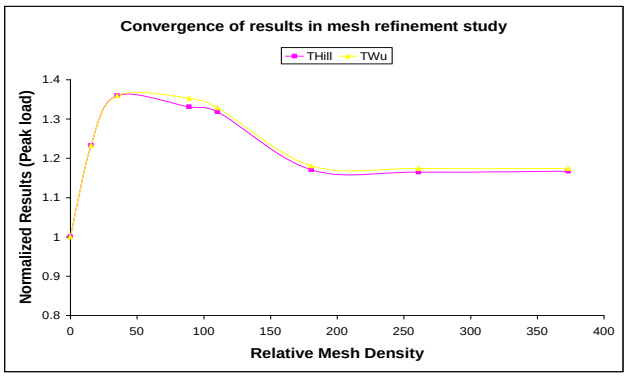

Figure 17: Convergence of results for peak load

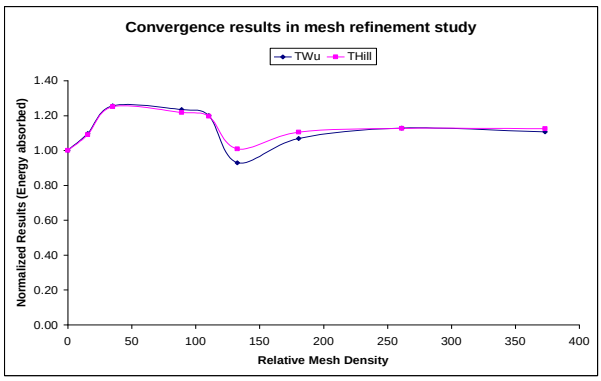

Figure 18: Convergence of results for energy absorbed

7. RESULTS AND DISCUSSIONS

The experimental crushing test was conducted on the glass/epoxy fuselage section to determine its peak load and its energy absorption by applying a lateral force onto the fuselage section such as shown schematically in figure 15. This was done using the MTS servo hydraulic machine. Next, a numerical simulation using ABAQUS finite element software was conducted and the results were validated with the experimental results. The correlation of the ABAQUS model of the composite

UAV fuselage section and the experimental result is shown in Figure 19 and Figure 20. The comparison of the simulated results using FE with the experimental data is made by plotting the crushing load per unit length–displacement history together with the crushing load per unit length –displacement history recorded during experiment (Fig. 20). Also shown is a comparison of the experimentally recorded deformation states and the deformation states obtained from the FE simulation (Fig. 19). The simulated and experimentally recorded data for the crushing of the laminated fuselage structure shows good agreement between the predicted and experimentally recorded deformation plots.

From the crushing load-displacement curves, the load per unit length and the energy absorbed can be determined via the crushing load divided by 0.2 meter length of the fuselage section and the area under the load-displacement curve equals the energy absorbed. The energy absorbed can be calculated by using equation (3).

$$W_P = \int_0^s P ds \tag{3}$$

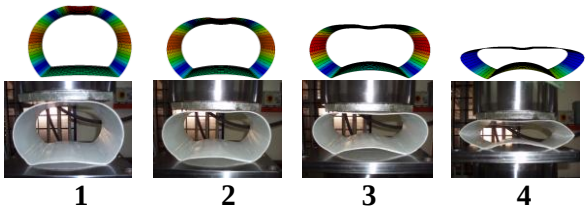

Figure 19: Comparison of deformation photos between simulation and experiment

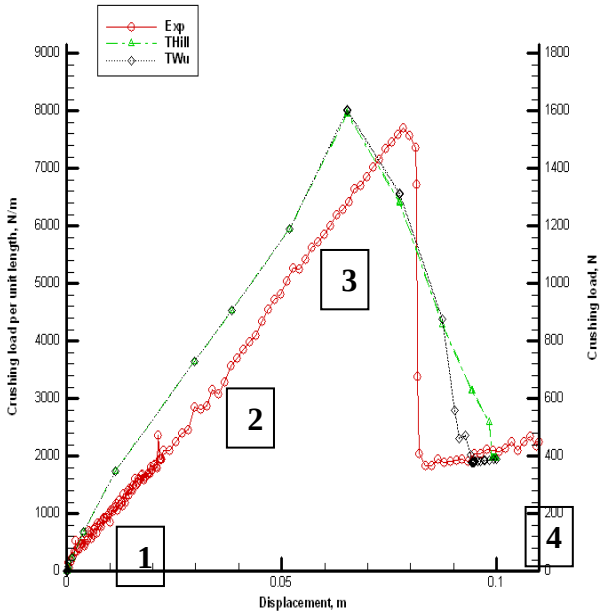

Figure 20: Crushing loading vs. Displacement

The agreement between the experiment and numerical results is found to be good throughout the loading process. At the beginning of the loading process, the applied load increases linearly up to the point where the maximum load is reached. After that, the experimental load-displacement curve and the simulated load-displacement curve drop off sharply. The error in percentage for the peak load between the experiment and the failure theories used to simulate the progressive damage is found to be 3.44% and 4.09% for Tsai-Hill Failure Theory and Tsai-Wu Failure Theory, respectively. It can be seen that Tsai-Hill and Tsai-Wu predict more or less the same as the experiment for the peak load. The error for Tsai-Hill and Tsai-Wu are 27.40% and 24.85% respectively when compared to the experiment for energy absorbed. These discrepancies between the results may be attributed to initial geometrical imperfections of the fuselage section during the lamination process which was not taken into account in the finite element analysis. In addition, the assumptions that $(\sigma^C{}_1)_{ult}$ equals $(\sigma^T{}_1)_{ult}$ and $(\sigma^C{}_2)_{ult}$ equals $(\sigma^T{}_2)_{ult}$ which have been made may also affect the results. Table 4 shows the comparison data for the experiment and the numerical results.

Table 4: Measured crashworthiness parameters for C-glass/epoxy 200g/m^2

	Peak load, N	Error, %	Energy Absorb, J	Error, %
Experiment	1540	0	69.16	0
Tsai-Hill	1593	3.44	88.11	27.40
Tsai-Wu	1603	4.09	86.35	24.85

8. CONCLUSION

An experimental and numerical quasi-static crush analysis of an unmanned aerial vehicle (UAV) fuselage section made of woven c-glass/epoxy has been successfully performed. A material characterization procedure has also been conducted to determine the mechanical properties of the woven c-glass-epoxy. These properties were then used as the input parameters in ABAQUS finite element package. The finite element analysis performed in this work employs the progressive damage methodology in order to simulate the non-linear material behaviour of the composite fuselage structure. This was achieved by linking a user subroutine USDFLD with the non-linear analysis using stress-based failure criteria, Tsai-Hill and Tsai-Hill.

It has been observed that the simulated peak load are found to agree with the experimentally recorded peak within an accuracy of 3.44% and 4.09% for Tsai-Hill and Tsai-Wu Failure criterion, respectively. On the other hand, the percentage errors between the experimental and

simulated crushing energy absorption are found to be 27.40% and 24.85% for Tsai-Hill and Tsai Wu theories respectively. This confirms the accuracy of the progressive damage methodology implemented in FE analysis for the woven glass/epoxy fuselage sections.

ACKNOWLEDGEMENT

The authors would like to thank University Putra Malaysia for providing a research fund for this project.

REFERENCES

ABAQUS 2003. ABAQUS User's manual, 1-3, Version 6.4. Pawtucket, RI:Hibbitt, Karlsson & Sorensen

ASTM D 3039/D 3039M – 95a, Standard Test Method for Tensile Properties of Polymer Matrix Composite

ASTM E 111 – 97, Standard Test Method for Young's Modulus, Tangent Modulus, and Chord Modulus.

ASTM E 1237 – 93, Standard Guide for Installing Bonded Resistance Strain Gages.

ASTM E 132 – 97, Standard Test Method for Poisson's Ratio at Room Temperature.

Hill, R. 1994. A theory of the yielding and plastic flow of anisotropic metals. Proceedings of the Royal Society of London, Series A, 281-297.

Jackson K.E. and Fasanella E.L. 1999. Crashworthy Evaluation of a 1/5-Scale Model Composite Fuselage Concept, 55th American Helicopter Society Annual Forum and Technology Display, Montreal, Canada, 25-27.

Jackson K.E. and Fasanella E.L. 1998a. Development of a 1/5 Scale Model Fuselage Concept for Improved Crashworthiness, Symposium on Size Effects and Scaling Laws, 13th U.S. National Congress on Applied Mechanics, Gainesville, FL, 21-26.

Jackson K.E. and Fasanella E.L. 1998b. Innovative Composite Fuselage Design for Improved Crashworthiness, 54th American Helicopter Society Forum and Technology Display, Washington DC, 20-22.

Jackson K.E. and Fasanella, E.L.. 1998c. Analytical and Experimental Evaluation of Composite Energy Absorbing Subfloor Concepts, Proceedings of the AHS National Technical Specialists' Meeting on Rotorcraft Crashworthiness, Phoenix, AZ, 14-17.

Jackson K.E. and Fasanella, E.L. 2000. Impact Testing and Simulation of a Crashworthy Composite Fuselage, 56th American Helicopter Society Annual Forum, Virginia Beach, Virginia, 2-4.

Jackson K.E. 1996. A Comparative Analysis of Three Composite Fuselage Concepts for Crash Performance, Proceedings of the 52nd AHS Forum and Technology Display, Washington DC, 4-6.

Jackson K.E. 1997. Analytical Crash Simulation of Three Composite Fuselage Concepts and Experimental Correlation, Journal of the American Helicopter Society, 42(2), 116-125.

Tsai, S.W. and Wu, E.M. 1971. A general theory of strength for anisotropic materials. Journal of Composite Materials, 5, 58-80